05,07

Crystal structure and piezoelectric and dielectric properties of a new series of solid solutions $SrBi_2Nb_{2-x}Ta_xO_9$ ($x = 0.0, 0.2, 0.4, 0.6, 0.8, 1.0$)

© S.V. Zubkov, Yu.A. Kuprina

Southern Federal University, Research Institute of Physics, Rostov-na-Donu, Russia

E-mail: svzubkov61@mail.ru

Received October 22, 2025
Revised October 22, 2025
Accepted October 24, 2025

Aurivillius–Smolensky (AS) ceramics $SrBi_2Nb_{2-x}Ta_xO_9$ ($x = 0.0$, 0.2, 0.4, 0.6, 0.8, 1.0), number of perovskite-like layers $n = 2$ were synthesized (for $x = 0.2$, 0.4, 0.6, 0.8, 1.0) by traditional solid-phase reaction. According to X-ray powder diffraction data, it was found that all compounds are single-phase with the structure of AS phases (number of perovskite-like layers $n = 2$) with an orthorhombic crystal lattice (space group $A2_1am$). The crystal lattice parameters a, b, and c were calculated, relative dielectric constant $\varepsilon/\varepsilon_0(T)$, dielectric loss tangent $\mathrm{tg}\,\delta$, Curie temperature T_C, and piezoelectric modulus d_{33} were measured.

Keywords: Aurivillius–Smolensky phases, Curie temperature, microstructure, dielectric constant, piezoelectric modulus.

DOI: 10.61011/PSS.2025.10.62636.290-25

1. Introduction

In 1949 when studying the system Bi_2O_3–TiO_2 V. Aurivillius found that $Bi_4Ti_3O_{12}$ oxide with a perovskite-type structure was formed [1]. Ten years later, the G. Smolenskii's group [2] discovered ferroelectric properties in $Bi_2PbNb_2O_9$ that belongs to this compound family, which was followed by an intense stage of investigation of these compounds. In this regard, these compounds can be rightfully called Aurivillius–Smolensky phases (ASP) [3]. In 1961–1962 E.S. Subbarao obtained about ten new compounds, almost all of them turned out to be ferroelectric [4,5]. As of now, hundreds of the ASPes are synthesized. They form a large family of bismuth-containing perovskite-type layered compounds, the chemical composition of which is described by the general formula $Bi_2A_{m-1}B_mO_{3m+3}$. ASP crystalline structure includes alternating layers of $[Bi_2O_2]^{2+}$, separated by m perovskite-like layers $[A_{m-1}B_mO_{3m+1}]^{2-}$, where A-positions are occupied by large-radius ions: Na^+ [6], K^+ [7], Ca^{2+} [8], Sr^{2+} [9], Ba^{2+} [10], Pb^{2+} [11], Y^{3+} [12,13], Bi^{3+}, La^{3+} [14], Nd [15], Sm [16], Gd [17], Ce [18], Tb [19], Dy [20], Ho [21], Er [22], Eu [23] and Ac, Th, Pr (actinides) which exhibit dodecahedral coordination. B-positions inside oxygen octahedra are occupied by highly charged ($\geq 3^+$) cations of small radius: Fe, Cr, Mn, Co [24–26], as well as Cu^{2+} [27], Mg^{2+} [28], Ti^{4+}, W^{6+} [29], Nb^{5+} [30], Ta^{5+} [31]. The value of m is determined by the number of perovskite layers m $[A_{m-1}B_mO_{3m+1}]^{2-}$ located between the fluorite-like layers $[Bi_2O_2]^{2+}$ along pseudo-diagonal axis c [32], and can be an integer or a half-integer [33] number in the range 1–5. Substitutions of atoms at positions A and B significantly affect the electrical properties of the ASP. There are large changes of permittivity and electrical conductivity; besides, the Curie temperature T_C can also vary widely. Thus, the study of the cation-substituted ASP compounds is of great importance in the development of materials for various technical purposes.

$SrBi_2Nb_2O_9$ (SBN) is one of the most promising candidates for non-volatile random access memory and resonators with frequency variation accuracy (about 15 %) [34–36].

Numerous studies have been conducted to improve the ferroelectric and piezoelectric properties of SBN ceramics by ion alloying [37,38]. The doping of Pr, Nd, and La positions of Bi in SBN leads to a relaxation behavior [39–41]. Also high piezoelectric constant $d_{33} \leq 20$ pC/N, low dielectric losses of SBN [42–45] and excellent tendency of a „no fatigue" [46–50] were reported.

This study is aimed at investigating the effect of isomorphic substitution on the piezoelectric properties of synthesized series of $SrBi_2Nb_{2-x}Ta_xO_9$ ($x = 0.0$, 0.2, 0.4, 0.6, 0.8, 1.0).

2. Experiment

The polycrystalline ASP series $SrBi_2Nb_{2-x}Ta_xO_9$ ($x = 0.0$, 0.2, 0.4, 0.6, 0.8, 1.0) was synthesized by a solid-state reaction of the appropriate oxides Bi_2O_3, $SrCO_3$, Ta_2O_5, Nb_2O_5. All the starting compounds were of AR (analytical reagent) grade. After weighing in a stoichiometric composition and thorough fining of the initial oxides with addition of ethanol, the pressed samples were ignited at the temperature of 860–870 °C during 4 h. The samples were

Table 1. Bond lengths in an oxygen octahedron for $SrBi_2Nb_{2-x}Ta_xO_9$

No.	Sample	$l(Nb_1-O_1)$	$l(Nb_2-O_2)$	$l(Nb_4-O_4)$	$l(Nb-O_5)$
1	$SrBi_2NbTaO_9$	2.1465	1.9295	2.0698	2.06287
2	$SrBi_2Nb_{1.2}Ta_{0.8}O_9$	2.1471	1.93101	2.0698	2.0623
3	$SrBi_2Nb_{1.4}Ta_{0.6}O_9$	2.144	1.9274	2.0698	2.0624
4	$SrBi_2Nb_{1.6}Ta_{0.4}O_9$	2.1455	1.92877	2.0698	2.0623
5	$SrBi_2Nb_{1.8}Ta_{0.2}O_9$	2.1437	1.9271	2.0709	2.065
6	$SrBi_2Nb_2O_9$	2.1456	1.9288	2.0698	2.0623

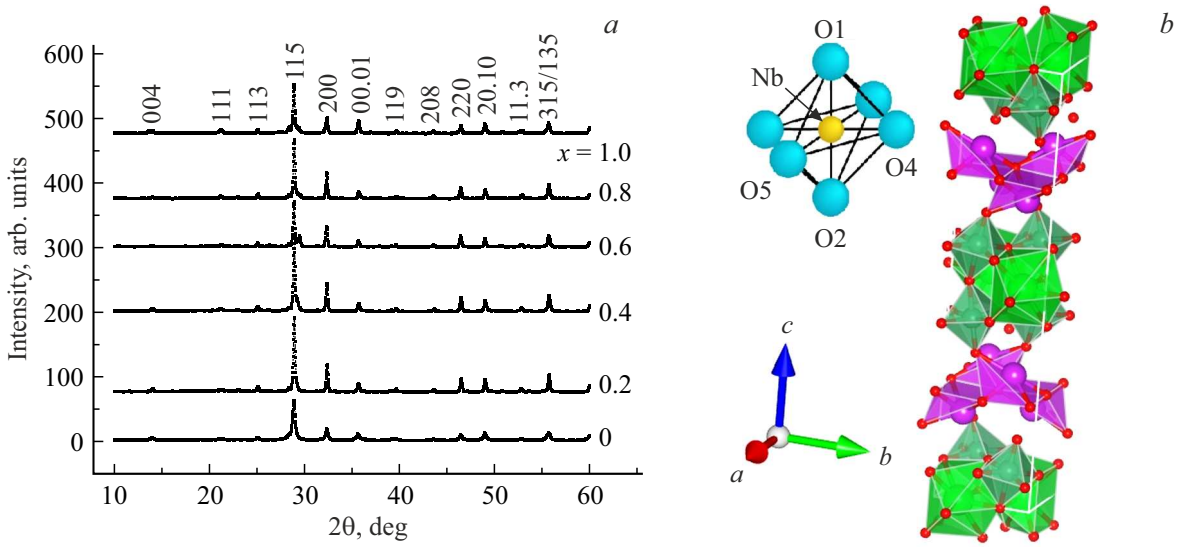

Figure 1. *a*) X-ray diffraction patterns of ceramics $SrBi_2Nb_{2-x}Ta_xO_9$ ($x = 0.0$, 0.2, 0.4, 0.6, 0.8, 1.0) within the frequency range 2θ 10−60°. *b*) Crystalline structure of $SrBi_2Nb_2O_9$ shown with the lattice and positional parameters in the oxygen octahedron.

calcinated in a muffle furnace in air. The sample was then crushed, repeatedly fined and pressed into pills of a diameter of 9 mm and a thickness 1.0−1.5 mm, with subsequent final synthesis at the temperature of 1140 °C (2 h). The X-ray image was recorded at a diffractometer Rigaku Ultima IV with a Cu X-ray tube. Radiation Cu K_{α_1,α_2} was picked up out of the general spectrum by means of a Ni filter. The X-ray image was measured in the angle range 2θ from 10 to 60° with a scanning step of 0.02° and an exposure (intensity registration time) of 4 s per point. The analysis of the X-ray profile, the determination of the position of the lines, their indexing (hkl) and the refinement of the structure were carried out by the Rietveld method in Full Prof Suitt program. In order to measure the permittivity and electric conductivity, electrodes were applied onto flat surfaces of the studied samples using Ag paste annealed at the temperature of 720 °C (20 min). The temperature and frequency characteristics of the dielectric characteristics were measured using E7-20 LCR meter in the frequency range from 100 kHz to 1 MHz and in the temperature range from the room temperature to 500 °C. The piezoelectric constantd_{33} was measured by polarizing the sample in an oil bath at 150 °C under voltage 45−65 kV/cm for 30 min. The values of the piezoelectric constant of the studied compounds were found from a relationship with the known value of the piezoelectric constant of a reference X-cut quartz sample.

3. Results and discussion

Powder X-ray diffraction patterns of all the studied solid solutions $SrBi_2Nd_{2-x}Nb_xO_9$ ($x = 0.0$, 0.2, 0.4, 0.6, 0.8, 1.0) correspond to the single-phase ASPes with $m = 2$ and have not additional reflections. These compounds are isostructural to the known perovskite-like oxide of the SBN ASP. All the peaks are indexed based on orthorhombic cells related to a space group $A2_1am$, which corresponds to JCPDS file of No. 49-0617 (No. 36 in PCW 2.4). Figure 1, *a* shows the experimental powder X-ray diffraction pattern of the studied compounds $SrBi_2Nb_{2-x}Ta_xO_9$ ($x = 0.0$, 0.2, 0.4, 0.6, 0.8, 1.0). The peak (115) in the X-ray diffraction

Table 2. Lattice cell parametersa_0, b_0, c_0, V, a_t — parameter of tetragonal period, c' — height of octahedron in c, axis $\delta c'$ — deviation from cube shape, δb_0 — rhombic distortion

No.	Sample	a_0, Å	b_0, Å	c_0, Å	c'	a_t	$\delta c'$	δb_0	V, Å^3
1	$SrBi_2NbTaO_9$	5.5103	5.513	25.0648	3.7686	3.9064	−3.52	0.235	761.425
2	$SrBi_2Nb_{1.2}Ta_{0.8}O_9$	5.5072	5.5142	25.0072	3.76365	3.9068	−3.66	0.216	759.413
3	$SrBi_2Nb_{1.4}Ta_{0.6}O_9$	5.5064	5.5168	25.0356	3.7674	3.9043	−3.5	0.345	760.275
4	$SrBi_2Nb_{1.6}Ta_{0.4}O_9$	5.5062	5.517	25.0537	3.7656	3.9046	−3.56	0.235	761.074
5	$SrBi_2Nb_{1.8}Ta_{0.2}O_9$	5.5109	5.5197	25.0317	3.767	3.905	−3.53	0.217	761.427
6	$SrBi_2Nb_2O_9$	5.5059	5.5167	25.054	3.768	3.904	−3.48	0.315	761.

pattern of Figure 1, *a* shows the highest intensity in the plane $(11(2m+1))$. This typical diffraction peak corresponds to a layered structure of SBN [51].

Table 1 shows the lengths of the Nb/Ta−O bonds for the series $SrBi_2Nb_{2-x}Ta_xO_9$ ($x = 0.0$, 0.2, 0.4, 0.6, 0.8, 1.0).

3.1. Crystal lattice

The X-ray diffraction data were used to determine parameters of the lattice cell (lattice constants a_0, b_0, c_0 and the volume V), which are listed in Table 2.

Table 2 shows the parameters of orthorhombic δb_0 and tetragonal $\delta c'$ deformation; the average tetragonal period is a_t, the average thickness of one perovskite-like layer is c', where $c' = 3c_0/(8+6m)$, $a_t = (a_0+b_0)/(2\sqrt{2})$ — average parameter of tetragonal period; a_0, b_0, c_0 — lattice periods; $\delta c' = (c'-a_t)/a_t$ — deviation of the cell from the cubic shape, that is, elongation or contraction of the cubic shape; $\delta b_0 = (b_0-a_0)/a_0$ — orthorhombic deformation [52,53]. A tolerance factor t was introduced by V.M. Goldschmidt [54] as a geometric criterion that determines a degree of stability and distortion of the crystal structure:

$$t = (R_A + R_O)/\sqrt{2}(R_B + R_O), \qquad (1)$$

where R_A and R_B are the radii of cations in the sublattice A and B, respectively; R_O is the ionic radius of oxygen. Obviously, the value of t has the same value for the entire range of synthesized compounds. In the present study, the tolerance factor was calculated taking into account the table of ion radii of R.D. Shannon [55] for the corresponding coordination numbers (CN): O^{2-} (CN = 6), $R_{O^{2-}} = 1.40$ Å; Ta^{5+} (CN = 12), $R_{Ta^{5+}} = 0.64$ Å; Nb^{5+} (CN = 12), $R_{Nb^{5+}} = 0.64$ Å. Shannon did not use the ion radius Bi^{3+} to coordinate with KH = 12. Therefore, its value was determined from the ion radius with CN = 6 ($R_{Bi^{3+}} = 1.17$ Å) multiplied by the approximation factor 1.179, then for Bi^{3+} (CN = 12) $R_{Bi^{3+}} = 1.38$ Å.

As can be seen from Table 2, $\delta c'$ has a negative value, which corresponds to „compressed" state of the octahedron in the perovskite layer [56,57].

Almost all cell parameters remain constant, which is expected with the isomorphic substitution of Nb by Ta.

3.2. Dielectric properties

Dependences of the relative permittivity $\varepsilon/\varepsilon_0$ and the dielectric loss angle tangent $\mathrm{tg}\,\delta$ on the temperature for ASP $SrBi_2Nb_{2-x}Ta_xO_9$ ($x = 0.0$, 0.2, 0.4, 0.6, 0.8, 1.0), the number of perovskite-like layers $n = 2$ are shown in Figures 2 and 3, respectively, at frequency values from 100 kHz to 1 MHz for ceramics, sintered at temperatures of 1140−1150 °C.

The maximum permittivity $\varepsilon/\varepsilon_0(T)$, corresponding to the ferroelectric-paraelectric phase transition, is clearly observed for the entire range of solid solutions $SrBi_2Nb_{2-x}Ta_xO_9$ ($x = 0.0$, 0.2, 0.4, 0.6, 0.8, 1.0), $n = 2$ at frequencies from 100 kHz to 1 MHz. For the series $SrBi_2Nb_{2-x}Ta_xO_9$ ($x = 0.2$, 0.4, 1.0), $n = 2$ the decrease in $\mathrm{tg}\,\delta$ almost in ten times compared to SBN may be observed, for this series $SrBi_2Nb_{2-x}Ta_xO_9$ ($x = 0.6$, 0.8) — in 2 times. A decrease $\mathrm{tg}\,\delta$ for the whole series $SrBi_2Nb_{2-x}Ta_xO_9$ ($x = 0.2$, 0.4, 0.6, 0.8, 1.0) may be explained by the decline in defects of the crystalline structure and, as a consequence, lower number of oxygen vacancies. The decrease in defects is due to the fact that the substitution of Nb by Ta makes the bonds (Ta,Nb)−O less covalent. Since 5*d*-orbital of Ta is longer than 4*d*-orbital of Nb, hybridization of 5*d*-orbital of Ta with O2*p* reduces the binding energy and makes the bond less covalent. Covalence is essential in structural distortions and ferroelectricity in ferroelectric oxides [58]. Thus, a decrease in the covalent interaction in the octahedral unit leads to a decrease in structural distortions and a lower in temperature Curie T_C.

For the whole series $SrBi_2Nb_{2-x}Ta_xO_9$ ($x = 0.2$, 0.4, 0.6, 0.8, 1.0) an absence of depression $\varepsilon/\varepsilon_0(T)$ over frequency is observed. For $\mathrm{tg}\,\delta$ $SrBi_2Nb_{2-x}Ta_xO_9$ ($x = 0.2$, 0.4) in the range $x = 0.2-0.4$ has no any usual dependence of the Curie temperature T_C and the minimum value $\mathrm{tg}\,\delta$ is observed (see Figure 3, *f* and *e*). In addition, there is a mixing of the minimum $\mathrm{tg}\,\delta$ towards higher values for $x = 0$

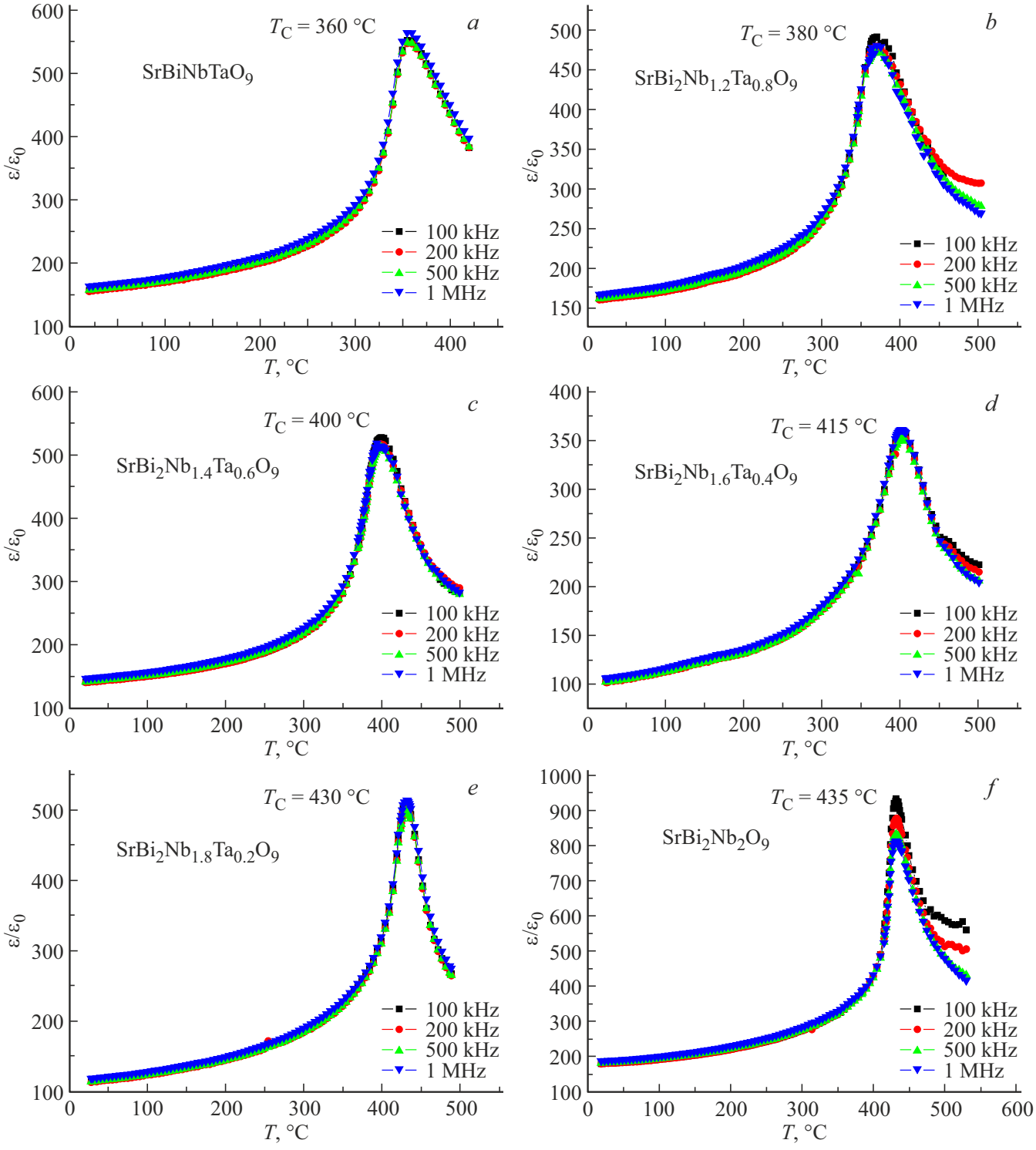

Figure 2. Temperature dependences of relative permittivity $\varepsilon/\varepsilon_0(T)$ for $SrBi_2Nb_{2-x}Ta_xO_9$ (x = 0.0, 0.2, 0.4, 0.6, 0.8, 1.0).

from the phase transition temperature, which may be an indirect sign of the relaxor properties of $SrBi_2Nb_2O_9$, on the one hand. On the other hand, the substitution of Nb by Ta at values of $x = 0.2$ is associated with a decrease in oxygen vacancies and lower dielectric losses. The fact that at a concentration of $x = 0.2$there is no substitution of Nb by Ta in the oxygen octahedron can be judged by a slight change in Curie temperature of $T_C = 435$ and 430 °C for $x = 0.0$ and 0.2 accordingly.

Table 3 gives the temperatures of phase transition T_C with the rise of parameter x. The Curie temperature T_C decreases almost linearly with increase of x.

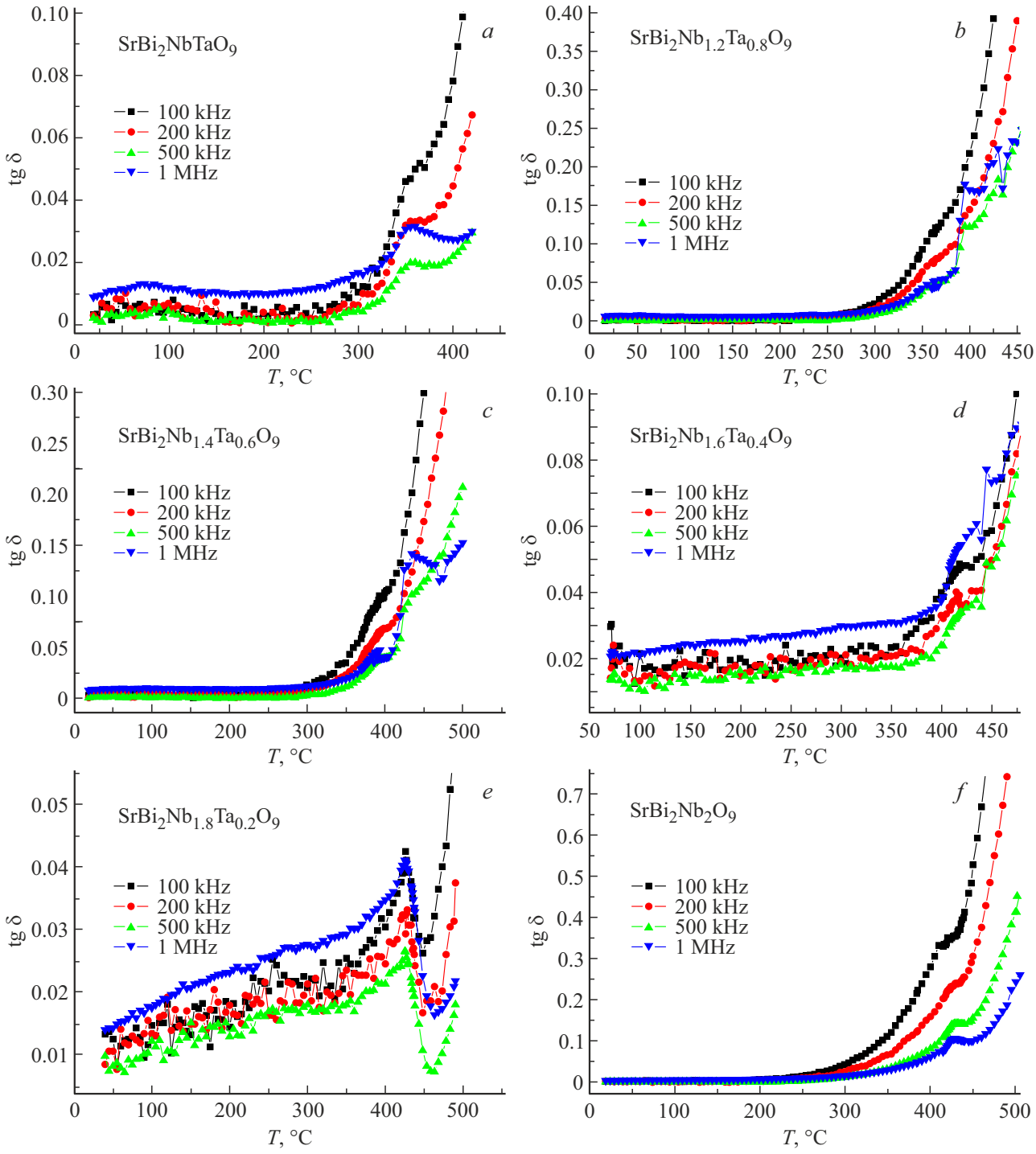

Figure 3. Temperature dependences of the dielectric loss angle tangent tg δ for $SrBi_2Nb_{2-x}Ta_xO_9$ ($x = 0.0$, 0.2, 0.4, 0.6, 0.8, 1.0).

As can be seen from Table 3, the temperature of the phase transition T_C exhibits an almost linear dependence on the parameter x.

3.3. Piezoelectric measurements

The piezoelectric constantd_{33} was measured by polarizing the sample in an oil bath at 150 °C under voltage 45–65 kV/cm for 30 min. The values of the piezoelectric constant of the studied compounds were found from a relationship with the known value of the piezoelectric constant of a reference X-cut quartz sample. The value of piezoelectric constant d_{33} for SBN stoichiometric ceramics was 14 pC/N and is in good agreement with the published values [59]. For $SrBi_2Nb_{2-x}Ta_xO_9$ ($x = 0.2$, 0.4, 0.6) the values of piezoelectric constant are within

Table 3. Curie temperature T_C, relative permittivity $\varepsilon/\varepsilon_0$ and loss tangent $\mathrm{tg}\,\delta$, measured at 100 kHz, piezoelectric constant d_{33}

No.	Composition	T_C, °C	$\varepsilon/\varepsilon_0$	d_{33}, pC/N	$\mathrm{tg}\,\delta$ (100 kHz)
1	$SrBi_2NbTaO_9$	360	580	14	0.05
2	$SrBi_2Nb_{1.2}Ta_{0.8}O_9$	380	490	12	0.14
3	$SrBi_2Nb_{1.4}Ta_{0.6}O_9$	400	528	17	0.1
4	$SrBi_2Nb_{1.6}Ta_{0.4}O_9$	415	360	16	0.05
5	$SrBi_2Nb_{1.8}Ta_{0.2}O_9$	430	513	17	0.04
6	$SrBi_2Nb_2O_9$	435	935	14	0.38

16–17 pC/N, for $SrBi_2Nb_{2-x}Ta_xO_9$ ($x = 0.8,\ 1.0$) — in the range 12–14 pC/N. The growth of the piezoelectric constant from 14 to 17 pC/N can be attributed to a lower amount of defects in the compounds and a decrease in the degree of covalence, and is completely unrelated to a decrease in the covalence of bonds in the oxygen octahedron.

4. Conclusions

The electrophysical properties of perovskite-like oxides AS of solid solutions $SrBi_2Nb_{2-x}Ta_xO_9$ were studied ($x = 0.0,\ 0.2,\ 0.4,\ 0.6,\ 0.8,\ 1.0$). The ceramic was made using the traditional method of solid-phase reaction. The X-ray diffraction patterns are indexed as orthorhombic $A2_1am$ for all the ASP solid solutions. Isomorphic substitution of Nb by Ta for $SrBi_2Nb_{2-x}Ta_xO_9$ ($x = 0.0,\ 0.2,\ 0.4,\ 0.6,\ 0.8,\ 1.0$) resulted in lowering the Curie temperature T_C by 75 °C, from 435 °C for $SrBi_2Nb_2O_9$ to 360 °C for $SrBi_2NbTaO_9$. The dielectric loss angle tangent decreased by 10 times for $SrBi_2Nb_{1.8}Ta_{0.2}O_9$ compared to unalloyed SBN. Obviously, lower $\mathrm{tg}\,\delta$ leads to increasing d_{33}.

Piezoelectric constant for the entire range of synthesized compounds $SrBi_2Nb_{2-x}Ta_xO_9$ ($x = 0.0,\ 0.2,\ 0.4,\ 0.6,\ 0.8,\ 1.0$) has a value from 12 to 17 pC/N, which allows us to conclude that the piezoelectric constant is independent of the degree of bond co-valence in the oxygen octahedron during isomorphic substitution.

Synthesized compounds of $SrBi_2Nb_{2-x}Ta_xO_9$ series ($x = 0.0,\ 0.2,\ 0.4,\ 0.6,\ 0.8,\ 1.0$) are candidates for high temperature piezoelectric applications.

Funding

The study was supported by the Ministry of Science and Higher Education of the Russian Federation [State assignment in the field of scientific activity 2023 project No. FENW-2023-0015).

Conflict of interest

The authors declare that they have no conflict of interest.

References

[1] B. Aurivillius. Arkiv. Kemi. **1**, *54*, 463 (1949).
[2] G.A. Smolensky, V.A. Isupov, A.I. Agranovskaya. Sov. Phys. Solid State **3**, *3*, 651 (1961).
[3] I.A. Parinov, S.V. Zubkov. J. Adv. Dielectr. **14**, *06*, 2340007 (2024).
[4] E.C. Subbarao. J. Am. Ceram. Soc. **45**, *4*, 166 (1962).
[5] E.C. Subbarao. J. Chem. Phys. **34**, *2*, 695 (1961).
[6] C. Long, Q. Chang, Y. Wu, W. He, Y. Li, H. Fan. J. Mater. Chem. **3**, *34*, 8852 (2015).
[7] W.S. Woo, S.S. Won, C.W. Ahn, S.A. Chae, A. Ullah, I.W. Kim. J. Appl. Phys. **115**, *3*, 034107 (2014).
[8] T. Li, X.L. Li, Z. Zhao, H. Ji, Y. Dai. J. Integr. Ferroelectr. **162**, *1*, 1 (2015).
[9] S.V. Zubkov, I.A. Parinov, A.V. Nazarenko, Y.A. Kuprina. Springer Proceed. Mater. **20**, 163 (2023).
[10] S. Dubey, O. Subohi, R. Kurchanic. Appl. Phys. A **124**, *7*, 461 (2018).
[11] S.V. Zubkov. J. Adv. Dielectrics **11**, *5*, 2160016 (2021).
[12] S.V. Zubkov, V.G. Vlasenko. Phys. Solid State **59**, *12*, 2325 (2017).
[13] Y. Li, C.J. Lu, J. Su, Y.C. Zhang, C. Zhang, S.F. Zhao, X.X. Wang, D.J. Zhang, H.M. Yin. J. Alloys. Compd. **687**, 707 (2016).
[14] J. Su, Y. Long, Q. Li, C. Lu, K. Liang, J. Li, L. Luo, L. Sun, X. Lu, J. Zhu. J. Alloys. Compd. **747**, 1002 (2018).
[15] D.L. Zhang, L. Feng, W. Huang, W. Zhao, X. Li. J. Appl. Phys. **120**, *15*, 154105 (2016).
[16] F. Rehman, L. Wang, H.-B. Jin, P. Ahmad, Y. Zhao, J.-B. Li. J. Alloys. Compd. **709**, 686 (2017).
[17] V. Koval, I. Skorvanek, G. Viola, M. Zhang, C. Jia, H. Yan. J. Phys. Chem. C **122**, *27*, 15733 (2018).
[18] P. Fang, P. Liu, Z. Xi, W. Long, X. Li. Mater. Sci. Eng. B **186**, 21 (2014).
[19] A. Faraz, J. Ricote, R. Jimenez, T. Maity, M. Schmidt, N. Deepak, S. Roy, M.E. Pemble, L. Keeney. J. Appl. Phys. **123**, *12*, 124101 (2018).
[20] Y. Qiu, S. Zhao, Z. Wang. Mater. Lett. **170**, 89 (2016).
[21] Y. Bai, J. Chen, S. Zhao. RSC Adv. **6**, *47*, 41385 (2016).
[22] D. Peng, H. Zou, C. Xu, X. Wang, X. Yao, J. Lin, T. Sun. AIP Adv. **2**, *4*, 042187 (2012).
[23] Z. Zhu, X. Li, W. Gu, J. Wang, H. Huang, R. Peng, X. Zhai, Z. Fu, Y. Lu. J. Alloys. Compd. **686**, 306 (2016).
[24] Y. Li, M. Bian, N. Zhang, W. Bai, J. Yang, Y. Zhang, X. Tang, J. Chu. Ceram. Int. **45**, *7 Part A*, 8634 (2019).
[25] H. Sun, T. Yao, X. Xie, Y. Lu, Y. Wang, Z. Xu, J. Han, X. Chen. J. Colloid. Interf. Sci. **534**, 499 (2019).
[26] Y. Shu, Q. Ma, L. Cao, Z. Ding, X. Chen, F. Yang. J. Alloys Compd. **773**, 934 (2019).
[27] H. Zhao, H. Wang, Z. Cheng, Q. Fu, H. Tao, Z. Ma, T. Jia, H. Kimura, H. Li. Ceram. Int. **44**, *11*, 13226 (2018).
[28] Y. Huang, L. Mi, J. Qin, S. Bi, H.J. Seo. J. Am. Ceram. Soc. **102**, *6*, 3555 (2019).
[29] X.Z. Zuo, J. Yang, B. Yuan, D.P. Song, X.W. Tang, K.J. Zhang, X.B. Zhu, W.H. Song, J.M. Dai, Y.P. Sun. J. Appl. Phys. **117**, *11*, 114101 (2015).
[30] F. Rehman, L. Wang, H.-B. Jin, A. Bukhtiar, R. Zhang, Y. Zhao, J.-B. Li. J. Am. Ceram. Soc. **100**, *2*, 602 (2017).
[31] H. Zou, J. Li, X. Wang, D. Peng, Y. Li, X. Yao. Opt. Mater. Express **4**, *8*, 1545 (2014).

[32] C.A. Paz de Araujo, J.D. Cuchiaro, L.D. McMillan, M.C. Scott, J.F. Scott. Nature **374**, *6523*, 627 (1995).
[33] T. Kikuchi. J. Less Common Met. **48**, *2*, 319 (1976).
[34] C.A. Paz de Araujo, J.D. Cuchiaro, L.D. McMillan, M.C. Scott, J.F. Scott. Nature **374**, *6523*, 627 (1995).
[35] D.P. Volanti, L.S. Cavalcante, E.C. Paris, A.Z. Simöes, D. Keyson, V.M. Longo, A.T. de Figueiredo, E. Longo, J.A. Varela, F.S. De Vicente, A.C. Hernandes. Appl. Phys. Lett. **90**, *26*, 261913 (2007).
[36] A. Ando, M. Kimura, Y. Sakabe. Jpn. J. Appl. Phys. **42**, *2R*, 520 (2003).
[37] S. Sen, R.N.P. Choudhary, P. Pramanik. Ferroelectrics **324**, *1*, 121 (2005).
[38] S.E. Park, J.A. Cho, T.K. Song, M.H. Kim, S.S. Kim, H.-S. Lee. J. Electroceram. **13**, *1*, 51 (2004).
[39] S. Huang, C. Feng, L. Chen, X. Wen. Solid State Commun. **133**, *6*, 375 (2005).
[40] S. Huang, C. Feng, M. Gu, Y. Li. J. Alloys. Compd. **472**, *1–2*, 262 (2009).
[41] L. Sun, C. Feng, L. Chen, S. Huang. J. Appl. Phys. **101**, *8*, 084102 (2007).
[42] R. Singh, V. Luthra, R.S. Rawat, R.P. Tandona. Ceram. Int. **l41**, 4468 (2015).
[43] B.J. Kennedy, Ismunandar. J. Mater. Chem. **9**, *2*, 541 (2006).
[44] P. Banerjee, A. Franco. Mater. Chem. Phys. **225**, 213 (2019).
[45] Y. Wu, M.J. Forbess, S. Seraji, S.J. Limmer, T.P. Chou, C. Nguyen, G. Cao. J. Appl. Phys. **90**, *10*, 5296 (2001).
[46] T. Wei, C.Z. Zhao, Q.J. Zhou, Z.P. Li, Y.Q. Wang, L.S. Zhang. Opt. Mater. **36**, *7*, 1209 (2014).
[47] V. Shrivastava. Ceram. Int. **42**, *8*, 10122 (2016).
[48] M. Nagata, D.P. Vijay, X. Zhang, S.B. Desu. Physica Status Solidi A **157**, *1*, 75 (1996).
[49] P. Banerjee, A. Franco. Physica Status Solidi **214**, *10*, 1700067 (2017).
[50] Y. Shimakawa, Y. Kubo, Y. Tauchi, T. Kamiyama, H. Asano, F. Izumi. Appl. Phys. Lett. **77**, *17*, 2749 (2000).
[51] X. Du, I.-W. Chen. J. Am. Ceram. Soc. **81**, *12*, 3253 (1998).
[52] V.A. Isupov. Ferroelectrics **189**, *1*, 211 (1996).
[53] V.A. Isupov. Inorg. Mater. **42**, *11*, 1236 (2006).
[54] V.M. Goldschmidt. Geochemische Verteilungsgesetze der Elemente. J. Dybwad, Oslo (1923−1927).
[55] R.D. Shannon. Acta Crystallographica A **32**, *5*, 751 (1976)
[56] T. Obata, T. Manako, Y. Shimakawa, Y. Kubo. Appl. Phys. Lett. **74**, *2*, 290 (1999).
[57] N.C. Hyatt, J.A. Hriljac, T.P. Comyn. Mater. Res. Bull. **38**, *5*, 837 (2003).
[58] R.E. Cohen. Nature **358**, *6382*, 136 (1992).
[59] X. He, R. Chu, Z. Xu, Z. Yao, J. Hao. RSC Adv. **8**, *28*, 15613 (2018).

Translated by T.Zorina